This article has been accepted for publication in IEEE Antennas and Wireless Propagation Letters. This is the author's version which has not been fully edited and content may change prior to final publication. Citation information: DOI 10.1109/LAWP.2022.3184758

Efficient Mutual-Coupling Aware Fault Diagnosis of Phased Array Antennas using Optimized Excitations

Prajosh K P, Sreekar Sai Ranganathan, Francesco Ferranti, *Senior Member, IEEE*, Uday K Khankhoje, *Senior Member, IEEE*

***Abstract*—Antenna fault diagnosis for phased antenna arrays is an important research area since faulty elements deteriorate the expected field pattern, leading to degraded performance in various applications. While several compressive sensing-based techniques have been proposed, they rely on a simplified array factor formula, ignoring mutual coupling effects among antennas. We show that this assumption can lead to poor diagnosis in the presence of significant mutual coupling by using two popular models – the average embedded element pattern and a port-level coupling matrix approach. Also, we optimize the antenna excitations to minimize the mutual coherence of the system measurement matrix, leading to a reduced number of measurements required for fault diagnosis. Our simulation results indicate that accounting for the effect of mutual coupling results in a far more reliable diagnosis. Additionally, our framework is executed using a single measurement probe fixed in space, thus making a step towards practical fault diagnosis techniques that can be deployed on antenna array systems.**

***Index Terms*—Phased arrays, Fault diagnosis, Signal processing, Optimization methods**

I. Introduction

PHASED ARRAY antennas play a vital role in applications such as remote sensing, radar, and wireless communications [1], [2], as well as in applications requiring high beam efficiencies with upper bounds on power patterns [3]. As a result, their proper functioning is fundamental for efficient operation. Faulty elements in a large antenna array can lead to undesired radiation patterns, resulting in degraded performance of the overall system. Therefore, locating the faulty elements and adopting necessary compensating/correction techniques are inevitable tasks for the robust operation of a phased array. Since the number of faults can be assumed to be small compared to the total number of elements, this enables the use of compressive sensing (CS) for fault diagnosis. Several works [4]–[13] have been proposed in the past for efficient fault diagnosis using CS, including some experimental validations [14]. In most of these techniques, diagnosis is performed by recovering a sparse solution from few far-field measurements at a few locations in space, which indicates the healthy or faulty status of the elements. More recent methods suggest that fault diagnosis can be performed using measurements from a fixed point in space with a sequence of array excitations [10], [11], [13]. In our recent work [13], optimizing the mutual coherence of the sensing matrix was introduced to improve the capability of diagnosis for a given number of fixed-probe measurements.

However, these techniques use a simplified far-field model based on the array factor. While this offers simplicity, ignoring non-idealities may be questionable for practical fault diagnosis, particularly when the spacing between elements is sub-wavelength. While recent works have been aimed at modeling the multi-path channel to the fixed probe in the presence of faults [15], [16], there are no works, to our knowledge, that addresses the influence of mutual coupling [17] among elements of the antenna array for fault diagnosis using a fixed receiver probe for measurements.

In this paper, we investigate how to incorporate mutual coupling in the fault diagnosis technique proposed in [13] and demonstrate that not accounting for coupling effects leads to poor fault diagnosis results. We show how the nature of our fault diagnosis approach of using a fixed probe *and* optimized excitations allows us to achieve optimal performance simply even while mutual coupling (using any method) is taken into account. We demonstrate numerical results involving average embedded element patterns and port-level coupling matrix approaches; these show that our approach effectively achieves a much more reliable fault diagnosis.

We note that while there have been previous work [18] attempting fault diagnosis in the presence of mutual coupling, they are based on measurements at multiple locations, and applicable to uniform linear arrays. Our method, in contrast, applies to more general array geometries and provides efficient fault diagnosis using measurements from a fixed location by optimizing the excitations. Further, two approaches for modeling mutual coupling effects are provided in this paper, which can be used depending on the antenna array's characteristics and the information available to the user about the antenna array.

Manuscript received Apr 16, 2022. (*Corresponding author: Uday Khankhoje*.)

The authors are with the Department of Electrical Engineering, Indian Institute of Technology Madras, Chennai, India. F Ferranti is also with the Department of Applied Physics and Photonics, Brussels Photonics, Vrije Universiteit Brussel, Brussels, Belgium. (e-mail: ee17d044@smail.iitm.ac.in; ee18b154@smail.iitm.ac.in; Francesco.Ferranti@vub.be; uday@ee.iitm.ac.in.)

II. Methods

A. Far Field of a Faulty Phased Array

It is known from the linearity of Maxwell's equations that the electromagnetic field emitted by a phased array system can be represented in terms of a linear combination of the excitations of the constituent antenna elements, i.e. $E(r) = \sum_{i=1}^{N} \alpha_i(r)\, x_i$, where $E(r)$ is the field at location r, the excitations are x_i, and the coefficients of the combination, $\alpha_i(r)$,

© 2022 IEEE. Personal use is permitted, but republication/redistribution requires IEEE permission. See https://www.ieee.org/publications/rights/index.html for more information.
Authorized licensed use limited to: INDIAN INSTITUTE OF TECHNOLOGY MADRAS. Downloaded on June 25,2022 at 04:29:54 UTC from IEEE Xplore. Restrictions apply.

This article has been accepted for publication in IEEE Antennas and Wireless Propagation Letters. This is the author's version which has not been fully edited and content may change prior to final publication. Citation information: DOI 10.1109/LAWP.2022.3184758

contain information about the electromagnetic environment of the element in the array and the measurement setup, and N is the number of array elements.

Since our objective is to perform fault diagnosis in the presence of mutual coupling between the elements, we now outline the mathematical steps that lead to a system model:

Modeling element faults: Here, we simply replace the excitation x_i by the expression $x_i\rho_i$, where $\rho_i \in \mathbb{C}$ captures the fault state of the element (e.g. $\rho_i = 1$ indicates no fault, whereas $\rho_i = 0$ indicated a dead element).

Modeling mutual coupling: In the simplest case, when the coupling is ignored (isolated element pattern approach), α_i consists of terms that quantify the element gain and the phase due to the path length between the measurement and antenna element locations. On the other end of the spectrum, if the α_i terms are computed using the embedded (or active) element patterns [19], then mutual coupling effects are fully taken into account at the cost of N full-wave electromagnetic simulations per measurement location. Various other techniques have been proposed in the literature, including "average" embedded patterns [20] and port-level, coupling matrix approaches [21], [22] (also see [23] for an excellent review).

Thus, while the details of the mutual coupling model can be changed as per the available computational resources, the mathematical expression for the measured field can be written as:

$$E(r) = \sum_{i=1}^{N} x_i \alpha_i(r) \rho_i, \tag{1}$$

where the definition of the α_i terms will depend on the specific model used for mutual coupling effects.

B. Fault Diagnosis Methodology

In recent work [13] we showed how fault diagnosis of a phased array could be accomplished utilizing a single probe fixed in space; multiple measurements are realized by optimally changing the element excitations. We generalize this result in our work by incorporating the previously ignored effect of mutual coupling between the antenna elements. Doing so makes the fault diagnosis technique very practical and relevant to phased arrays with sub-wavelength inter-element spacing.

On examining (1), we observe that as long as the measurement location is fixed, the α_i terms do not change (henceforth we drop the 'r' argument on α). Leveraging this observation, we build a vector of M measurements, $\tilde{y}$, and relate it to the excitations as: $\tilde{y}_i = \sum_{j=1}^{N} x_j^{(i)} \alpha_j \rho_j$, where $x_j^{(i)}$ is the excitation of element-j for measurement-i, which in turn leads to the following succinct system model:

$$\tilde{y} = \begin{bmatrix} x^{(1)} \\ \vdots \\ x^{(M)} \end{bmatrix} \begin{bmatrix} \alpha_1 & 0 & 0 \\ 0 & \ddots & 0 \\ 0 & 0 & \alpha_N \end{bmatrix} \begin{bmatrix} \rho_1 \\ \vdots \\ \rho_N \end{bmatrix} = \underbrace{X \mathrm{diag}(\alpha)}_{B} \rho, \tag{2}$$

where $x^{(i)} \in \mathbb{C}^{1\times N}$ consists of the element excitations for the i^{th} measurement, resulting in an overall excitation matrix, $X \in \mathbb{C}^{M\times N}$, and $\rho \in \mathbb{C}^{N\times 1}$ is the fault-state vector.

As is common in fault diagnosis methodology, we assume that a reference set of measurements, say $y^{(R)}$, are available for a known set of element states, $\rho^{(R)}$ (typically corresponding to a fault-free array). If we further assume that the number of faults with respect to this reference is *sparse*, then after forming the differential measurement vector $y = y^{(R)} - \tilde{y}$, the optimization problem to solve for fault diagnosis is:

$$\min_z \|z\|_0, \text{ s.t. } \|y - Bz\| < \epsilon, \; z = \rho^{(R)} - \rho, \tag{3}$$

where ϵ is a parameter proportional to the standard deviation of measurement noise.

To recover a sparse solution, it is desirable that the sensing matrix B has low mutual coherence [24], [25]. In [13], the excitation matrix X is optimized for mutual coherence by approximating a Grassmannian matrix using an alternating procedure [24], which shows improved performance when compared to a randomized X [26]. Since B is defined as a diagonal matrix multiplied by X, the mutual coherence of the matrix B will be the same as that of X, thus allowing us to optimize the mutual coherence oblivious to the type of antenna mutual coupling model used. The key intuition here is that the linear coupled forward model remains the same for different excitations. It is important to note that this would not have been possible if multiple locations were being used for measurements.

Most fault diagnosis techniques formulate (3) as an ℓ_1 minimization problem, while others use a non-convex ℓ_p $(0 < p < 1)$ minimization approach [7], [11]–[13] due to its superior performance. By standard methods we convert (3) into an unconstrained nonconvex optimization problem [13]:

$$\min_z \|y - Bz\|_2^2 + \eta \|z\|_p^p, \; 0 < p < 1, \tag{4}$$

where η is an empirical hyperparameter. This is solved using Iterative Reweighted ℓ_1 minimization (IRL1) [27], [28] implemented using the Alternating Direction Method of Multipliers (ADMM) [29].

III. Results

We consider a 7×7 dipole array in the $x - y$ plane (see Fig. 1), where the dipoles are oriented along an angle of 45° in-plane. The maximum of the field pattern is along the z-direction when uniform excitations are applied. Each dipole of length 0.47λ has a resonant frequency of 3 GHz, with a radius equal to $\frac{\lambda}{150}$ and is excited through a generator impedance of 50 Ω. The choice of dipole orientation is motivated by two considerations: (1) to prevent physical overlap of the elements at low values of inter-element spacing, e.g. for $d = 0.45\lambda$, and (2) to have a broadside radiation pattern commonly used in wireless systems.

We now present fault diagnosis results from the complex electric field (E_y) measurements at a fixed measurement position using optimized excitations. The field measurements of healthy and faulty arrays (i.e. the α_i's of the forward models in (1)) of the isolated pattern approach (based on the array factor approach [1]), average embedded pattern approach (based on [20, Eq. (11)]), and the coupling matrix approach

© 2022 IEEE. Personal use is permitted, but republication/redistribution requires IEEE permission. See https://www.ieee.org/publications/rights/index.html for more information.
Authorized licensed use limited to: INDIAN INSTITUTE OF TECHNOLOGY MADRAS. Downloaded on June 25,2022 at 04:29:54 UTC from IEEE Xplore. Restrictions apply.

This article has been accepted for publication in IEEE Antennas and Wireless Propagation Letters. This is the author's version which has not been fully edited and content may change prior to final publication. Citation information: DOI 10.1109/LAWP.2022.3184758

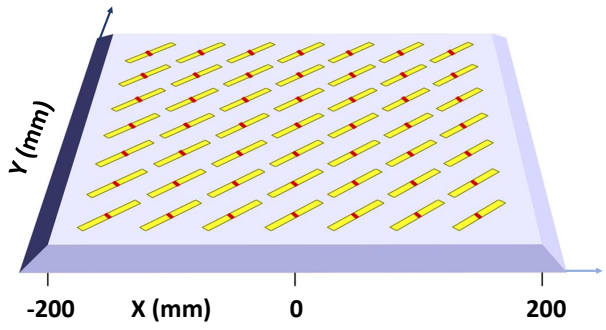

Fig. 1. Square 7×7 array of center fed dipoles in the $x-y$ plane.

(based on [22, Eq. (A9)]) were simulated using the MATLAB-Antenna toolbox. We highlight that the choice of the mutual coupling model is not restricted to the ones used in this work. Any mutual coupling models can be used by computing the appropriate α_i terms, due to general formulation of our framework (as per (2)).

The measurement location was fixed at a spherical angular location $(\theta_0, \phi_0) = (0, 0)$ with $r = 1000\lambda$ (along the z-axis). The fault solution using these measurements is obtained using IRL1. We fix the hyperparameters η in (4) $\eta = 0.25\|B^H y\|_\infty$ and $p = 0.3$ (p quasi-norm) for all the simulation results of fault diagnosis presented in this paper. The value of η is obtained empirically from a grid search performed from $0.1\|B^H y\|_\infty$ to $\|B^H y\|_\infty$, where the upper limit $\|B^H y\|_\infty$ is discussed in [24]. The amplitude and phase of the excitations are restricted to the interval $[0, 1]$ and $[0, 2\pi]$, respectively. The excitations (both random and optimized) are quantized to 6-bit amplitude and phase and the random excitations are generated from a multinomial probability distribution.

The recovered solution is mapped to binary values by thresholding the real part by 0.5, i.e. for the n^{th} element $\rho_n = 1$ if the reconstructed fault state is greater than 0.5, else $\rho_n = 0$. Fault recovery is considered a success when an exact reconstruction of the number of faulty elements and their location is achieved. We note that the thresholding operation is not necessary in case we are to deal with non-binary faults. We report our results in the rate of successful recovery (RSR) metric, the percentage of realizations that lead to successful recovery, and is calculated over 400 Monte-Carlo simulations with randomized fault locations. We now outline our primary findings.

A. Improvement in fault diagnosis by optimizing excitations

As stated earlier, our methodology can seamlessly incorporate the effects of mutual coupling. This means that we should expect a similar performance improvement as in [13] when using optimized excitations w.r.t. random excitations. We validate this by analyzing the performance of fault diagnosis using the coupling matrix model, with and without optimization of the excitation matrix X at an SNR of $10\,\text{dB}$; the plots in Fig. 2 indicate that the optimization of the excitation matrix X is indeed useful when using the coupling matrix approach. Similar results were obtained using the average embedded pattern approach as the mutual coupling model.

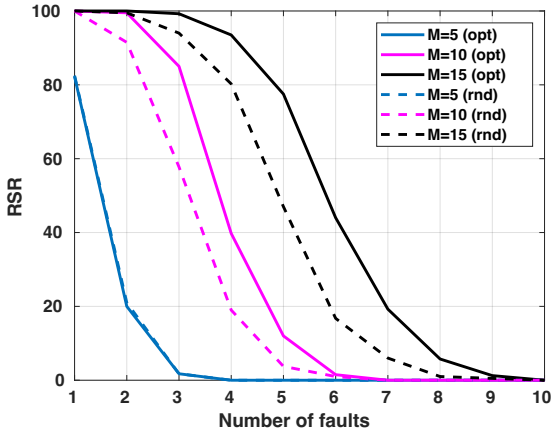

Fig. 2. RSR plot for the coupling matrix approach using IRL1, $N = 49$ (dipole array), $d = 0.45\lambda$ at 10 dB SNR.

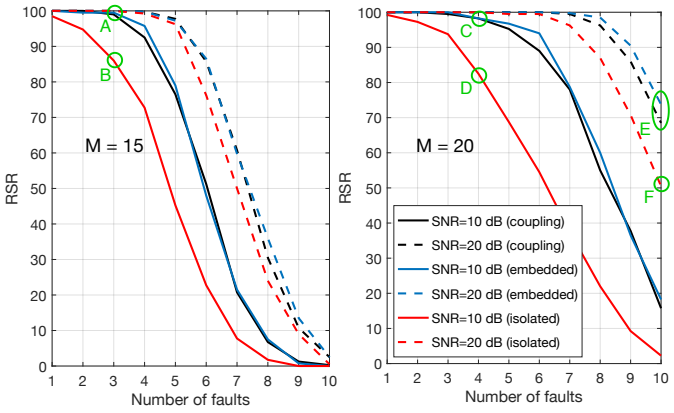

Fig. 3. RSR plot using IRL1, $N = 49$ (dipole array), d=0.45λ, and optimized excitations for two different number of measurements, $M = 15$ (left), $M = 20$ (right) with a shared legend.

This is a crucial finding: *all the advantages of the optimized element excitation approach [13] continue to apply* when mutual coupling effects are taken into account. Similar results are seen at higher SNR values, with a general improvement in the RSR at any given number of faults.

B. Improvement in fault diagnosis by incorporating coupling

Fig. 3 shows the RSR (in %age) against number of faults for recovery using the different coupling models using IRL1 and optimized excitations at SNR of $10\,\text{dB}$ and $20\,\text{dB}$, respectively. The RSR is plotted against the number of faults for two different numbers of measurements, M, and we see that:

1) In both cases, a clear improvement in the reliability of fault diagnosis is seen when coupling effects are taken into account. For example, at $10\,\text{dB}$ and $M = 15$ measurements with 3 faults, an RSR of 100 is achieved when coupling is taken into account, as opposed to an RSR of 85 when not (points A, B in Fig. 3). Similarly, at $10\,\text{dB}$ and $M = 20$ measurements with 4 faults, an RSR of 98 is achieved when coupling is taken into account, as opposed to an RSR of 83 when not (points C, D in Fig. 3).

© 2022 IEEE. Personal use is permitted, but republication/redistribution requires IEEE permission. See https://www.ieee.org/publications/rights/index.html for more information.
Authorized licensed use limited to: INDIAN INSTITUTE OF TECHNOLOGY MADRAS. Downloaded on June 25,2022 at 04:29:54 UTC from IEEE Xplore. Restrictions apply.

This article has been accepted for publication in IEEE Antennas and Wireless Propagation Letters. This is the author's version which has not been fully edited and content may change prior to final publication. Citation information: DOI 10.1109/LAWP.2022.3184758

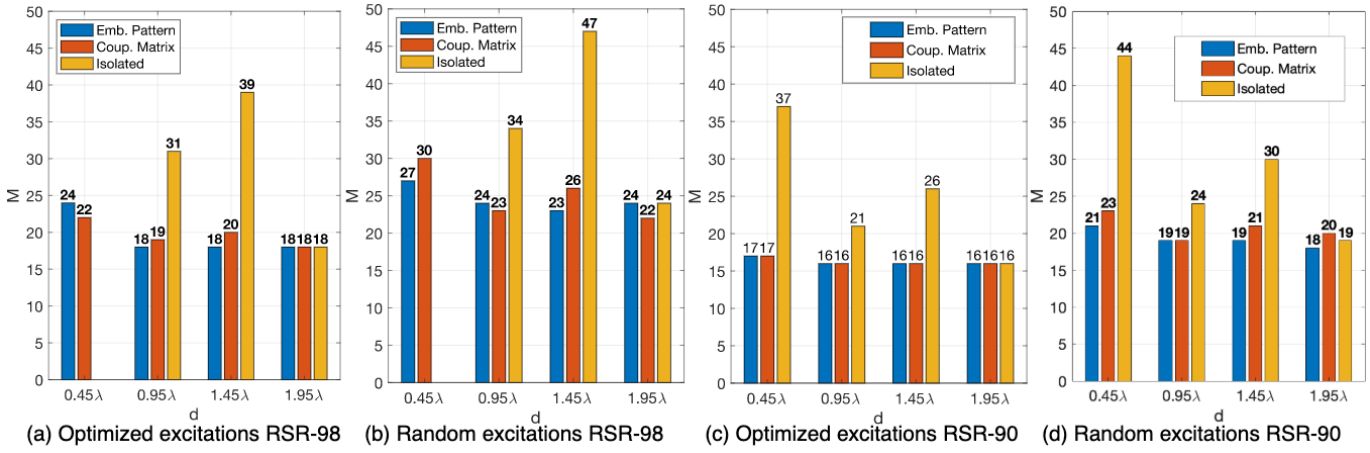

Fig. 4. Minimum number of measurements M required to reach RSR-98 (a,b) and RSR-90 (c,d) with varying d for 5 faults in a 49-element array for optimized (a,c) and random (b,d) excitations. The bars are unavailable for some cases, when the given RSR is not achieved for any $M \leq N$, i.e. the case where more measurements than total element number are required.

2) The difference in accuracy (RSR value) when accounting for mutual coupling is more significant when using low SNR measurements, seen for e.g. by contrasting the behavior of solid (low SNR) v/s dashed (high SNR) lines in Fig. 3: the dashed lines are more bunched up than the solid lines. In the case of high SNR, an improvement in RSR by taking mutual coupling into account is seen at larger fault numbers. For e.g. at $20\,\mathrm{dB}$ and $M = 20$ measurements with 10 faults, the isolated pattern approach achieves an RSR of 50 %, whereas coupling aware models achieve $\approx$ 70% RSR (regions E, F in Fig. 3).

C. Analysis with varying inter-element spacing

As the effect of mutual coupling is more significant when the antennas are closer, it is natural to expect that all the approaches should converge to a similar performance at higher inter-element spacing. As we demonstrate with our results, this is true in terms of the minimum number of measurements required for successful fault diagnosis.

The bar diagrams given in Fig. 4 show the number of measurements M needed to reach RSR-98 & RSR-90 when fault diagnosis is performed for different inter-element spacings using the proposed models and optimized/random excitations. The number of faults is fixed as 5, and SNR is set to $10\,\mathrm{dB}$. Among the bar diagrams shown in Fig 4, the lowest number of measurements for fault diagnosis (i.e. most efficient diagnosis) are obtained when using optimized excitations (see Figs. 4(a), & 4(c)). Some of the other important takeaways include the following:

1) The average embedded pattern and coupling matrix models clearly outperform the isolated pattern approach at any inter-element spacing. Moreover, the minimum required M to reach RSR-90 is nearly the same for these models, irrespective of the spacing.
2) The number of measurements needed for all the different models is almost the same at larger spacing ($d = 1.95\lambda$), where we expect minimum mutual coupling.
3) The difference between the coupling models and the isolated pattern model increases with decreasing inter-element spacing d, and the isolated pattern model fails to achieve RSR-98 at small inter-element spacing ($d = 0.45\lambda$) for any number of measurements $M < N(= 49)$.

Overall, the coupling matrix and the average embedded pattern models (with optimized excitations) are shown to be the best choices for fault detection in this example. However, it is essential to note here that the coupling matrix approach assumes that the impedance matrix of the array is available to the user. If unavailable, the average embedded pattern model may be suitable in a practical scenario with a sufficiently large array since it needs only the embedded pattern response of the center element, which is relatively easier to obtain.

IV. Conclusion

This paper presents two strategies to incorporate the effect of mutual coupling for efficient fault diagnosis of an antenna array using a novel compressive sensing technique that uses measurements from a fixed probe and optimized excitations. Depending on the information available about the antenna array and its characteristic properties, either of these strategies can be used. When the array is sufficiently large, the average embedded pattern approach is a suitable forward model choice, while the coupling matrix approach is valid for a specific class of antennas. We have demonstrated the superior performance of the forward models, which account for mutual coupling effects and highlight the inadequacy of a forward model that does not include these effects. Our novel method has been validated and is shown to be very accurate and efficient in identifying faults in antenna arrays where coupling effects cannot be neglected.

References

[1] R. C. Hansen, *Phased Array Antennas*. John Wiley & Sons, 2009.
[2] W. Hong, K.-H. Baek, and S. Ko, "Millimeter-wave 5G antennas for smartphones: Overview and experimental demonstration," *IEEE Transactions on Antennas and Propagation*, vol. 65, no. 12, pp. 6250–6261, Dec. 2017.

© 2022 IEEE. Personal use is permitted, but republication/redistribution requires IEEE permission. See https://www.ieee.org/publications/rights/index.html for more information.
Authorized licensed use limited to: INDIAN INSTITUTE OF TECHNOLOGY MADRAS. Downloaded on June 25,2022 at 04:29:54 UTC from IEEE Xplore. Restrictions apply.

This article has been accepted for publication in IEEE Antennas and Wireless Propagation Letters. This is the author's version which has not been fully edited and content may change prior to final publication. Citation information: DOI 10.1109/LAWP.2022.3184758

[3] A. F. Morabito, A. R. Laganà, and T. Isernia, "Optimizing power transmission in given target areas in the presence of protection requirements," *IEEE Antennas and Wireless Propagation Letters*, vol. 14, pp. 44–47, 2014.

[4] M. D. Migliore, "A Compressed Sensing Approach for Array Diagnosis From a Small Set of Near-Field Measurements," *IEEE Transactions on Antennas and Propagation*, vol. 59, no. 6, pp. 2127–2133, Jun. 2011.

[5] G. Oliveri, P. Rocca, and A. Massa, "Reliable diagnosis of large linear arrays—A Bayesian compressive sensing approach," *IEEE Transactions on Antennas and Propagation*, vol. 60, no. 10, pp. 4627–4636, Oct. 2012.

[6] M. D. Migliore, "Array diagnosis from far-field data using the theory of random partial Fourier matrices," *IEEE Antennas and Wireless Propagation Letters*, vol. 12, pp. 745–748, 2013.

[7] T. Ince and G. Ögücü, "Array failure diagnosis using nonconvex compressed sensing," *IEEE Antennas and Wireless Propagation Letters*, vol. 15, pp. 992–995, 2015.

[8] A. F. Morabito, R. Palmeri, and T. Isernia, "A Compressive-Sensing-Inspired Procedure for Array Antenna Diagnostics by a Small Number of Phaseless Measurements," *IEEE Transactions on Antennas and Propagation*, vol. 64, no. 7, pp. 3260–3265, Jul. 2016.

[9] B. Fuchs, L. Le Coq, and M. D. Migliore, "Fast antenna array diagnosis from a small number of far-field measurements," *IEEE Transactions on Antennas and Propagation*, vol. 64, no. 6, pp. 2227–2235, Jun. 2016.

[10] M. E. Eltayeb, T. Y. Al-Naffouri, and R. W. Heath, "Compressive sensing for millimeter wave antenna array diagnosis," *IEEE Transactions on Communications*, vol. 66, no. 6, pp. 2708–2721, Jun. 2018.

[11] C. Xiong, G. Xiao, Y. Hou, and M. Hameed, "A Compressed Sensing-Based Element Failure Diagnosis Method for Phased Array Antenna During Beam Steering," *IEEE Antennas and Wireless Propagation Letters*, vol. 18, no. 9, pp. 1756–1760, Sep. 2019.

[12] W. Li, W. Deng, Q. Yang, X. Zhang, J. Zhang, and M. D. Migliore, "A Hybrid Method for Array Diagnosis Using Random Perturbation-Convex Local Minimizer," in *2019 IEEE Radar Conference (RadarConf)*, Apr. 2019, pp. 1–5.

[13] K. P. Prajosh, U. K. Khankhoje, and F. Ferranti, "Element excitation optimization for phased array fault diagnosis," *Journal of Electromagnetic Waves and Applications*, vol. 35, no. 1, pp. 39–50, Jan. 2021.

[14] S. Costanzo, A. Borgia, G. Di Massa, D. Pinchera, and M. D. Migliore, "Radar array diagnosis from undersampled data using a compressed sensing/sparse recovery technique," *Journal of Electrical and Computer Engineering*, vol. 2013, no. 627410, Jan. 2013.

[15] R. Sun, W. Wang, L. Chen, G. Wei, and W. Zhang, "Blind diagnosis for millimeter-wave large-scale antenna systems," *IEEE Communications Letters*, vol. 25, no. 7, pp. 2390–2394, 2021.

[16] G. Medina, A. S. Jida, S. Pulipali, R. Talwar, N. A. J, T. Y. Al-Naffouri, A. Madanayake, and M. E. Eltayeb, "Millimeter-Wave Antenna Array Diagnosis with Partial Channel State Information," in *ICC 2021 - IEEE International Conference on Communications*, Jun. 2021, pp. 1–5.

[17] I. Gupta and A. Ksienski, "Effect of mutual coupling on the performance of adaptive arrays," *IEEE Transactions on Antennas and Propagation*, vol. 31, no. 5, pp. 785–791, Sep. 1983.

[18] Y. Zhang and H. Zhao, "Failure diagnosis of a uniform linear array in the presence of mutual coupling," *IEEE Antennas and Wireless Propagation Letters*, vol. 14, pp. 1010–1013, 2015.

[19] A. Ludwig, "Mutual coupling, gain and directivity of an array of two identical antennas," *IEEE Transactions on Antennas and Propagation*, vol. 24, no. 6, pp. 837–841, Nov. 1976.

[20] D. Kelley and W. Stutzman, "Array antenna pattern modeling methods that include mutual coupling effects," *IEEE Transactions on Antennas and Propagation*, vol. 41, no. 12, pp. 1625–1632, Dec. 1993.

[21] T. Su and H. Ling, "On modeling mutual coupling in antenna arrays using the coupling matrix," *Microwave and Optical Technology Letters*, vol. 28, pp. 231–237, Feb. 2001.

[22] B. Clerckx, C. Craeye, D. Vanhoenacker-Janvier, and C. Oestges, "Impact of Antenna Coupling on 2 x 2 MIMO Communications," *IEEE Transactions on Vehicular Technology*, vol. 56, no. 3, pp. 1009–1018, May 2007.

[23] C. Craeye and D. Gonzalez-Ovejero, "A review on array mutual coupling analysis," *Radio Science - RADIO SCI*, vol. 46, Apr. 2011.

[24] M. Elad, *Sparse and Redundant Representations: From Theory to Applications in Signal and Image Processing*, 1st ed. Springer Publishing Company, Incorporated, 2010.

[25] E. Candes and J. Romberg, "Sparsity and incoherence in compressive sampling," *Inverse Problems. An International Journal on the Theory and Practice of Inverse Problems, Inverse Methods and Computerized Inversion of Data*, vol. 23, no. 3, p. 969, Apr. 2007.

[26] E. J. Candes and T. Tao, "Near-optimal signal recovery from random projections: Universal encoding strategies?" *IEEE transactions on information theory*, vol. 52, no. 12, pp. 5406–5425, Nov. 2006.

[27] Q. Lyu, Z. Lin, Y. She, and C. Zhang, "A comparison of typical p minimization algorithms," *Neurocomputing*, vol. 119, pp. 413–424, Nov. 2013.

[28] S. Foucart and M.-J. Lai, "Sparsest solutions of underdetermined linear systems via q-minimization for 0\textless q$\leqslant$ 1," *Applied and Computational Harmonic Analysis*, vol. 26, no. 3, pp. 395–407, May 2009.

[29] S. Boyd, N. Parikh, E. Chu, B. Peleato, J. Eckstein *et al.*, "Distributed optimization and statistical learning via the alternating direction method of multipliers," *Foundations and Trends® in Machine learning*, vol. 3, no. 1, pp. 1–122, Jul. 2011.

© 2022 IEEE. Personal use is permitted, but republication/redistribution requires IEEE permission. See https://www.ieee.org/publications/rights/index.html for more information.
Authorized licensed use limited to: INDIAN INSTITUTE OF TECHNOLOGY MADRAS. Downloaded on June 25,2022 at 04:29:54 UTC from IEEE Xplore. Restrictions apply.